

Mechanism of Corrosion and Corrosion Inhibition of Tin in Aqueous Solutions Containing Tartaric Acid

Rabab M. El-Sherif* and Waheed A. Badawy

Chemistry Department, Faculty of Science, Cairo University, Gamaa Street, 12613 Giza, Egypt.

*E-mail: rabab1774@yahoo.com

Received: 8 August 2011 / Accepted: 31 October 2011 / Published: 1 December 2011

The electrochemical behavior of tin metal in tartaric acid solutions of different concentrations was investigated. Some amino acids, namely, alanine, glycine, glutamic acid and histidine were used as environmentally safe inhibitors for the tin dissolution process. Different electrochemical techniques including, potentiodynamic polarization and electrochemical impedance spectroscopy (EIS) were used. The metal surface was examined via scanning electron microscopy (SEM). The E/I curves showed that the anodic behavior of tin exhibits active/passive transition. The active dissolution of tin was increased by increasing tartaric acid concentration. Glycine was found to give the highest corrosion inhibition efficiency at a concentration of 0.02 mol dm^{-3} . The corrosion inhibition process is based on the adsorption of the amino acid molecules on the metal surface. The adsorption process was found to obey the Freundlich isotherm, and the adsorption of glycine on Sn has an adsorption free energy of -10.2 kJ/mol which reveals physical adsorption of the amino acid molecules on the metal surface. The experimental impedance data are in good agreement with the polarization experiments. An equivalent circuit model was proposed for fitting of the experimental impedance data, and to simulate the electrode/electrolyte interface.

Keywords: Amino acids, corrosion, impedance, tartaric acid, tin

1. INTRODUCTION

Tin is a moderately corrosion resistant material that is widely used in tinplate for food beverage [1]. The electrochemical behavior of tin in aqueous solutions is of interest due to the widespread technological application in soft solders, bronze and dental amalgam beside its use as tinplate [2-4]. Tinplate is light gauge, cold reduced, low carbon steel, coated with commercially pure tin. It possesses the strength and formability of steel and corrosion resistance and lustrous of tin. Worldwide, more than 9×10^{10} food packaging cans are used; therefore this application is by far the largest of its diverse industrial applications. About one third of the world's tin production goes into the manufacture of

tinplate [1, 5]. It provides robust form of packaging, allowing minimization of head space oxygen and sterilization of the foodstuff within the hermetically sealed can, giving long, safe ambient shelf life with minimal use of preservatives. The presence of bare tin surface inside the can leads to protection of the food flavor and its natural appearance through the oxidation of the tin surface in preference to oxidative degradation of the food. This process is vital for the long shelf life of the food cans, since this oxidation step passivates the tin surface preventing its corrosion [6]. Dissolution of metallic tin, especially from the inside of a can body into the food content has a major influence on the food quality and may cause toxicological effects. The presence of citric and tartaric acid in food beverage leads to the preferential formation of tin complexes and tin dissolution. The presence of oxidizing agents or depolarizers enhances the tin dissolution process by direct chemical attack without hydrogen evolution [4, 5]. Although organotin complexes have diverse toxicological profiles, inorganic tin complexes are assigned to be as essentially non-toxic [6]. Passivation of tin in the presence of carboxylic acids present in fruit juices and different foodstuffs was investigated [4, 7-10]. The oxidative degradation of tartaric acid, being the strongest naturally occurring acid in fruits, especially in grapes, has a harmful effect on the food beverage [11]. Such oxidative degradation is enhanced in the presence of Fe(II) coming from the tin dissolution and the corrosion of the mild steel sheets of the tinplate. The commonly present oxidation states of tin in aqueous solutions are the metal itself, Sn(0), the divalent cation, Sn(II), and the tetravalent cation, Sn(IV). The dissolution process is taking place as Sn(II) [4, 12]. Fortunately, the dissolution of tin in most cases is accompanied by an oxidation step to form a passive film that can protect the metal surface from further corrosion. The thickness of the passive film and its stability is dependent mainly on its formation conditions [8, 13].

Since tinplate has a vital importance for the canned food industry, the electrochemical behavior, especially the dissolution process and surface oxidation of tin seems to be an important subject worthy of intensive investigations. In this work, the corrosion and passivation behavior of tin in aqueous solutions containing tartaric acid, being a natural additive in food cans, was investigated. The control of the corrosion process by the addition of small amounts of amino acids as environmentally safe corrosion inhibitors was also investigated. In this respect, conventional electrochemical techniques and electrochemical impedance spectroscopy were used. Whenever it was necessary, the metal surface was investigated by scanning electron microscopy.

2. EXPERIMENTAL

Spectroscopically pure tin rod (Aldrich-Chemie) was used for the preparation of the working electrodes. The metal rod was mounted into glass tubes by two-component epoxy resin leaving a surface area of 0.31 cm^2 to contact the solution. The electrochemical cell was a three-electrode all-glass cell, with a platinum counter electrode and a silver-silver chloride reference electrode. Before each experiment, the working electrode was polished mechanically using successive grades emery papers down to 2000 grit, rubbed with a smooth polishing cloth, then washed with triple distilled water and transferred quickly to the electrochemical cell. The electrochemical measurements were carried out in aqueous solutions, where analytical grade reagents and triple distilled water were always used.

The electrochemical experiments were carried out using the Zahner Elektrik IM6 electrochemical workstation. For impedance measurements, the amplitude of the superimposed AC-signal was 10 mV peak to peak. The method involves direct measurements of the impedance, Z , and the phase shift, θ , of the electrochemical system in the frequency range from 0.1 to 10^5 Hz. The impedance measurements were performed for different immersion time intervals. To achieve reproducibility, each experiment was carried out at least three times. Unless otherwise stated, all experiments have been carried out at room temperature $25 \pm 1^\circ\text{C}$ and the potentials were measured against and referred to the silver/silver chloride reference electrode ($E^\circ = 0.2225$ V vs. NHE). Details of the experimental procedures and preparations were as described elsewhere [14-16].

Small additions of naturally occurring amino acids were used to inhibit the corrosion process of tin in tartaric acid solutions. It is well known that sulfur and sulfur-containing amino acids like cysteine react with metallic tin with the formation of tin complexes [17]. The amino acids used as environmentally safe inhibitors for the tin corrosion in tartaric acid solutions include two aliphatic acids, glycine and alanine, an acidic amino acid, glutamic acid and a basic amino acid, histidine. The pH of the solution, being an important factor in the corrosion process [11], was controlled using an ORION pH meter model 230A and was found to be 1.8 in 1.0 mol dm^{-3} tartaric acid and decreases to 1.5 in the presence of the amino acid. The corrosion inhibition efficiency, σ , was calculated from the measured values of the corrosion current densities measured in amino acid free and amino acid containing tartaric acid solutions. A JEOL JEM-100S electron microscope was used for the SEM surface analysis.

3. RESULTS AND DISCUSSION

3.1 Potentiodynamic measurements

Fig.1 presents the potentiodynamic measurements of tin electrode in aqueous tartaric acid solutions of different concentrations.

The figure shows the different oxidation steps of the metal surface. The potential was swept anodically from -2.5 V up to 2.5 V (Ag/AgCl) at a scan rate of 50 mV s^{-1} . As the potential gets more positive, the cathodic current density corresponding to hydrogen evolution reaction decreases until it reaches zero at a potential of ≈ -1.0 V. At more anodic potential ≥ -1.4 V an active dissolution region is recorded, which is characterized by an anodic current peak that depends on the tartaric acid concentration. This region extends over a range of potential which is also dependent on the acid concentration. The increase of the dissolution peak current, i_p , with the increase of tartaric acid concentration was found to obey a logarithmic law of the form:

$$i_p = a + b \log C \quad (1)$$

where a is the intercept of the i_p vs. $\log C$ linear relation (cf. Fig. 2) and b is the slope. The intercept, a , was found to be 22.5 mA cm^{-2} at 1.0 mol dm^{-3} tartaric acid. The value of b represents the rate of change of the peak current density with $\log C$.

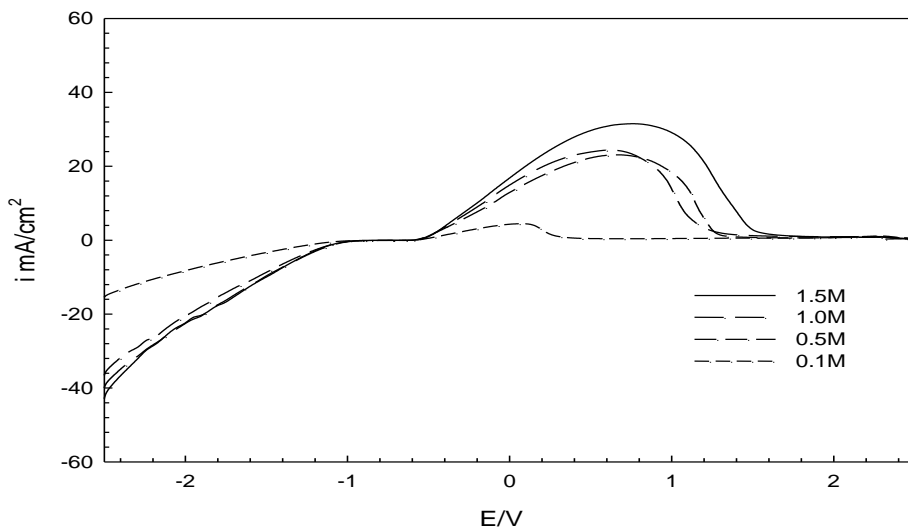


Figure 1. Potentiodynamic polarization curves of Sn electrode in naturally aerated aqueous tartaric acid solutions of different concentrations at pH 1.8 and 25°C . The scan rate is 50 mV s^{-1} .

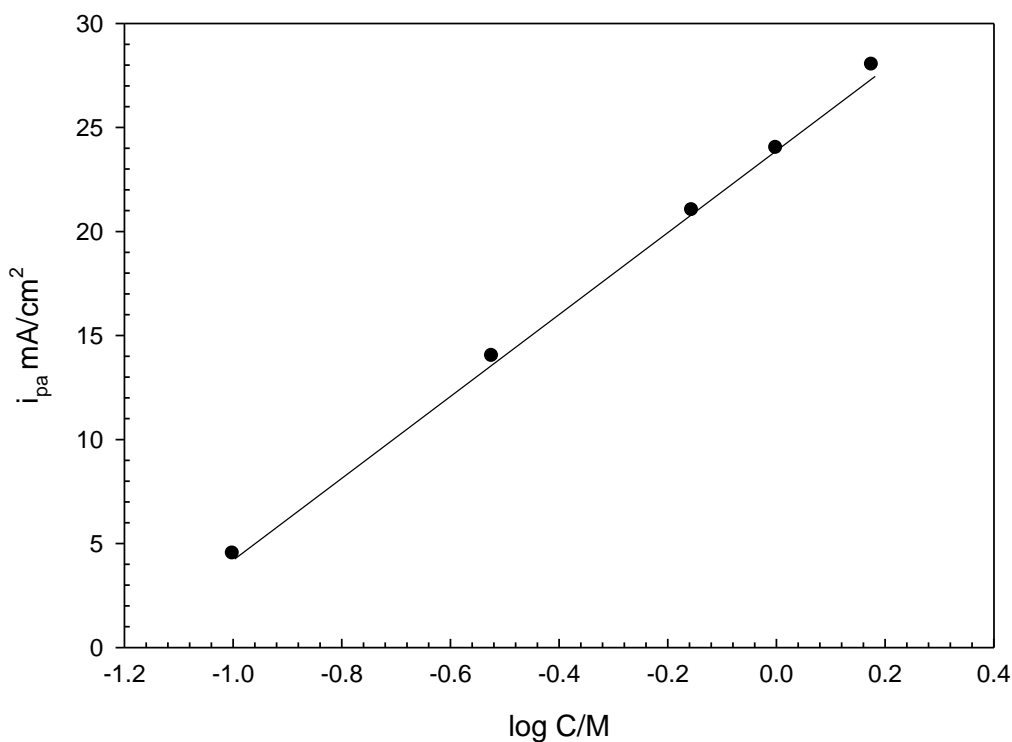
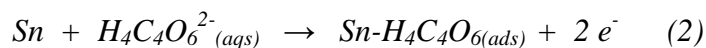


Figure 2. Relation between i_{pa} and $\log C_{acid}$ for Sn in naturally aerated aqueous tartaric acid solutions of pH 1.8 and 25°C .

The increase of i_p with the increase in the tartaric acid concentration can be explained by the adsorption tendency of the tartarate ion on the tin surface followed by the dissolution of the adsorbed complex according to:



At more anodic potentials the peak current diminishes and a passive region appears which extends from $\approx +1.8$ V up to $+2.5$ V and no oxygen evolution was recorded. This means that a passive film is formed, even in the acidic medium (pH 0.5-1.8), which is a poor electroconductor, whose formation and thickening were mainly caused by ionic conductance [18]. The dissolution of tin proceeds via the divalent cation according to the redox reaction:



At more anodic potentials, the Sn (II) species oxidize to the Sn (IV) according to:



The Sn (IV) species hydrolyze, even in acidic solutions [20], to give the hydroxide according to:



The formed hydroxide transforms into the hydrated tin oxide, $\text{SnO}_2 \cdot \text{H}_2\text{O}$, which is responsible for the recorded passivity [21, 22]. The dehydration of $\text{Sn}(\text{OH})_4$ to SnO_2 involves a free energy change of about -42 kJ mol^{-1} and is therefore an irreversible process [23]. Precipitation of tin oxide on the anode surface blocks the active surface sites and causes the recorded passive behavior.

3.2. Electrochemical Impedance Spectroscopic Measurements

The potentiodynamic experiments were confirmed by electrochemical impedance spectroscopy (EIS), which is a powerful technique in studying corrosion mechanisms and adsorption phenomena [24]. The technique enables the simulation of the experimental impedance results to theoretical data according to proposed electrical models representing the metal/solution interface. The fitting of the data can verify or rule out mechanistic models and enables the calculation of numerical values corresponding to physical and/or chemical properties of the system under investigation [16, 25]. Fig. 3 presents the impedance characteristics of the tin electrode after immersion in tartaric acid solutions for different time intervals. The data are presented as Bode plots, since this format is always recommended

as impedance plots. In such data presentation, all impedance results are equally represented and the phase angle, θ , being a sensitive parameter for interfacial phenomena, appears explicitly [24, 26]. In Fig. 3, there is a single phase maximum at all time intervals and the total impedance, Z , acquires a constant value at both high and low frequencies.

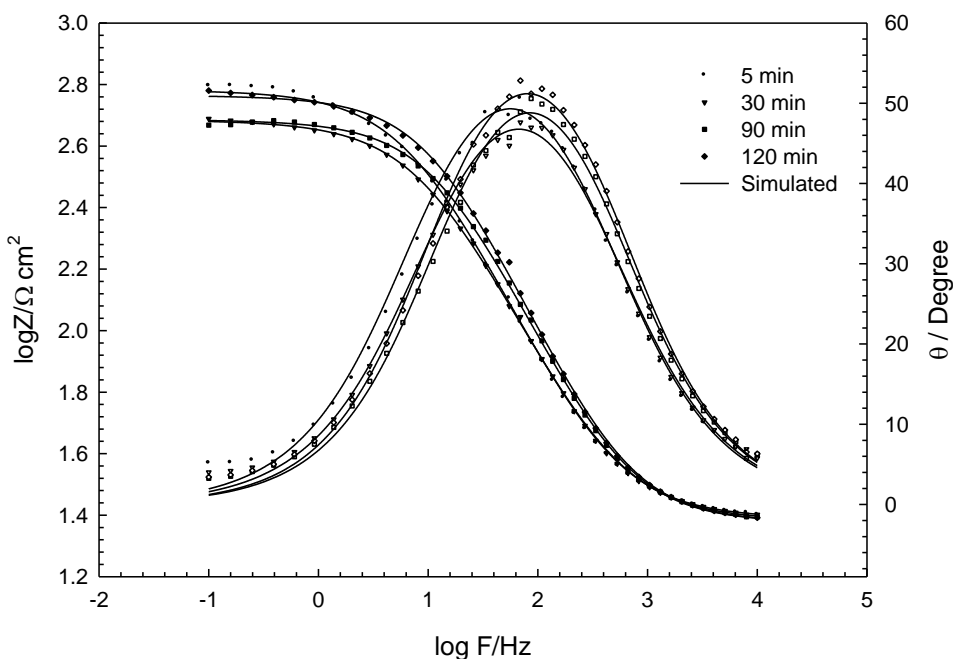


Figure 3. Bode plots for Sn electrode after different time intervals of immersion in naturally aerated aqueous 1.0 mol dm⁻³ tartaric acid solution at pH 1.8 and 25°C.

This means that the electrode process is governed by a single time constant i.e. it represents a simple corrosion process [14, 26]. The impedance data were analyzed using software provided with the electrochemical workstation, where the dispersion formula was used.

$$Z = R_s + R_{ct} / 1 + (2\pi f R_{ct} C_{dl})^\alpha \quad (7)$$

In this formula an empirical factor α ($0 \leq \alpha \leq 1$) is introduced to account for the deviation from the ideal capacitive behavior due to surface inhomogeneities, roughness factors and adsorption effects [16, 27, 28]. The experimental impedance values were fitted to a simple equivalent circuit model consisting of a parallel combination representing the electrode capacitance, C_{dl} , and the corrosion resistance, R_{ct} , in series with a resistor, R_s , representing the ohmic drop in the electrolyte (cf. Fig. 4). The equivalent circuit parameters were calculated and presented in Table 1.

The value of R_{ct} is in the range of 450 to 700 Ω , indicating the formation of a slightly passive layer as recorded by the potentiodynamic experiments. The calculated value of α is in the range of 0.75 to 0.8 which means that the passive layer thus formed deviates from the ideal RC behavior [29]. The

electrode capacitance, C_{dl} is in the range of 10 to 12 $\mu\text{F cm}^{-2}$, which is the value of normal double layer capacitance [24].

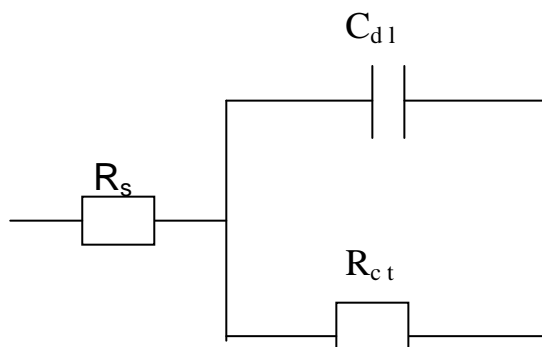


Figure 4. Equivalent circuit model for fitting of the experimental impedance data of Sn in naturally aerated aqueous tartaric acid solutions of pH 1.8 and 25°C. [R_s = solution resistance, R_{ct} = charge transfer (corrosion) resistance, C_{dl} = electrode capacitance].

Table 1. Equivalent circuit parameters for Sn after immersion in 1.0 mol dm⁻³ aqueous tartaric acid solution for different time intervals at 25°C.

Time (min)	R_s (Ω)	R_{ct} ($\text{k}\Omega \text{ cm}^{-2}$)	C_{dl} ($\mu\text{F cm}^{-2}$)	α
5	78.87	0.58	12.47	0.77
15	78.78	0.71	11.82	0.77
30	77.48	0.46	12.13	0.76
60	77.07	0.58	11.10	0.79
90	76.29	0.46	10.89	0.79
120	76.55	0.56	10.45	0.80

3.3. Effect of amino acids

The effect of different amino acids on the electrochemical behavior of tin after 2 h immersion in aqueous solutions containing 1.0 mol dm⁻³ tartaric acid was investigated by both the polarization and EIS techniques.

Different concentrations of glycine were added to the corrosive medium to optimize the most suitable concentration that leads to the lowest corrosion rate. The results of these experiments are summarized in Table 2. It is clear that the presence of 0.02 mol dm⁻³ of the amino acid is a suitable low concentration for the corrosion inhibition process. The effect of the same concentration of the different amino acids on the corrosion rate of tin was investigated using the Tafel polarization technique and presented as Tafel plots in Fig. 5. The values of the corrosion parameters and corrosion inhibition efficiency were calculated and presented in Table 3. In general, the presence of amino acids has a little

effect on the general shape of the polarization curves (cf. Fig. 5). The extrapolated corrosion current density is affected by the nature of the amino acid (cf. Table 3).

Table 2. Tafel slopes, E_{corr} , i_{corr} and the corrosion inhibition efficiency, σ , for Sn Electrode after 2 h immersion in 1.0 mol dm^{-3} aqueous tartaric acid solution containing different concentrations of glycine at 25°C .

[Glycine] ($1 \times 10^{-3} \text{ mol dm}^{-3}$)	β_a (mV/decade)	β_c (mV/decade)	E_{corr} (mV)	i_{corr} ($\mu\text{A cm}^{-2}$)	σ
0	58.3	-550	-497.1	64.50	-
1	65.8	-547	-499.9	52.25	19.0%
10	56.2	-425	-500.6	30.45	52.8%
20	55.2	-274	-513.8	19.60	69.6%
50	50.0	447	-512.0	24.60	61.8%
100	57.0	-293	-532.0	21.50	66.6%

Table 3. Tafel slopes, E_{corr} , i_{corr} and the corrosion inhibition efficiency, σ , for Sn electrode after 2 h immersion in 1.0 mol dm^{-3} aqueous tartaric acid solution containing 0.02 mol dm^{-3} of the different amino acids at 25°C .

[Amino Acid]	β_a (mV/decade)	β_c (mV/decade)	E_{corr} (mV)	i_{corr} ($\mu\text{A cm}^{-2}$)	σ
0.0	58.3	-550	-497.1	64.50	-
Glycine	55.2	-274	-513.8	19.60	69.6%
Alanine	59.3	-531	-511.8	40.00	37.9%
Histidine	68.4	-401	-514.0	41.90	35.0%
Glutamic acid	60.1	-366	-504.0	39.35	38.9%

A small molecule like glycine [$\text{CH}_2(\text{NH}_2)\text{COOH}$] gives the highest corrosion inhibition efficiency. The inhibition efficiency, σ , is calculated using the following equation:

$$\sigma = [(i - i_{\text{inh}}) / i] \times 100 \quad (8)$$

where, i and i_{inh} are the corrosion current densities before and after the corrosion inhibition process, respectively.

The inhibition effect of amino acid is due to the adsorption of its molecules on the metal surface [30]. In general, the amino acid molecule occurs in its protonated form in acidic solution according to:

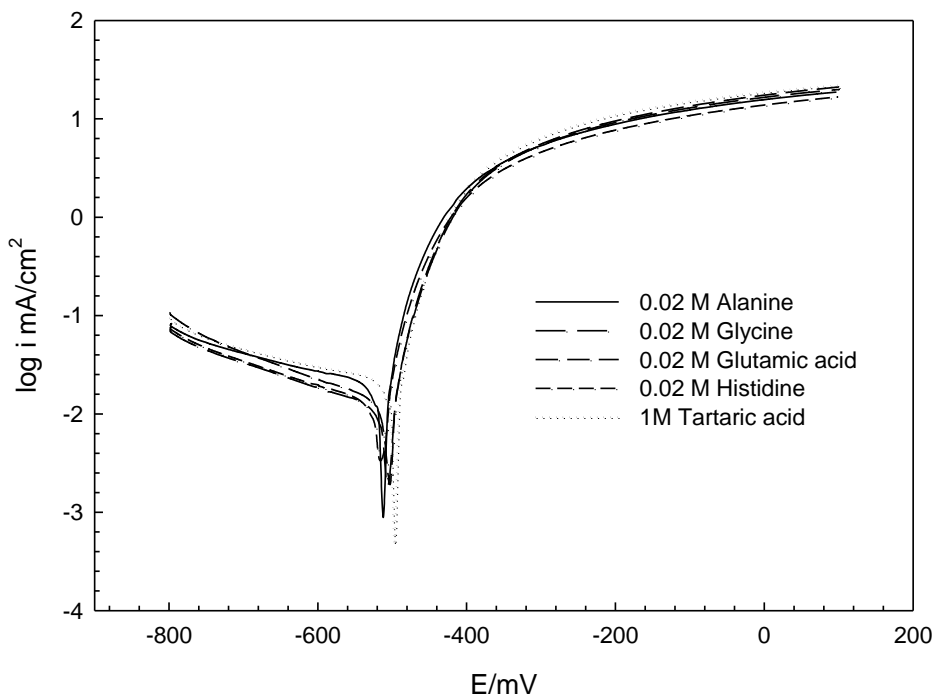
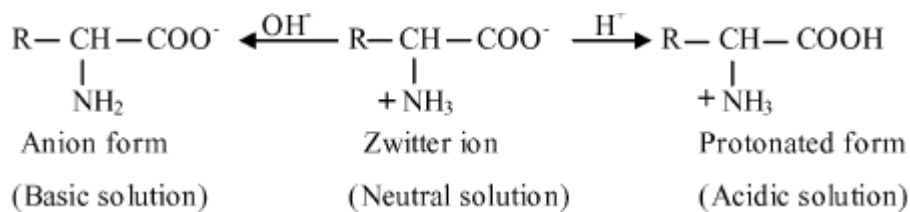


Figure 5. Potentiodynamic polarization curves of Sn electrode after 2 h immersion in amino acid free and 0.02 mol dm⁻³ amino acid containing tartaric acid (1.0 mol dm⁻³) solutions at 25°C.

It could be electrostatically attracted to the cathodic sites on the metal surface [30]. The effectiveness of the different amino acids as corrosion inhibitors is related to the extent of the adsorption of their molecules and how these molecules can cover the metal surface and protect it from continuous corrosion. The adsorption process depends on the structure of the inhibitor molecules, the surface charge of the metal, and the constituents of the electrolyte [31]. The relatively high inhibition efficiency of glycine compared to the other amino acids can be attributed to the higher tendency of glycine to be adsorbed on the active sites of tin inhibiting the adsorption of tartaric acid and the dissolution of the tin-tartrate complex according to equations 2 and 3. The effect of different amino acids was also investigated by EIS. Fig. 6 presents the Bode plots after 2 h of electrode immersion in aqueous solutions of 1.0 mol dm⁻³ tartaric acid containing 0.02 mol dm⁻³ of the amino acid. The impedance data were fitted to theoretical data according to the model of Fig. 4 and the equivalent circuit parameters were calculated and presented in Table 4. It is clear that the value of R_{ct} in the presence of glycine is more than triple its value in the case of the other amino acids (cf. Table 4). Also, the value of α becomes nearer to 1, which means that the electrode/electrolyte interface approaches the

RC behavior. Since the corrosion inhibition process is based on the adsorption of the amino acid molecules on the metal surface, it was important to study the adsorption phenomenon.

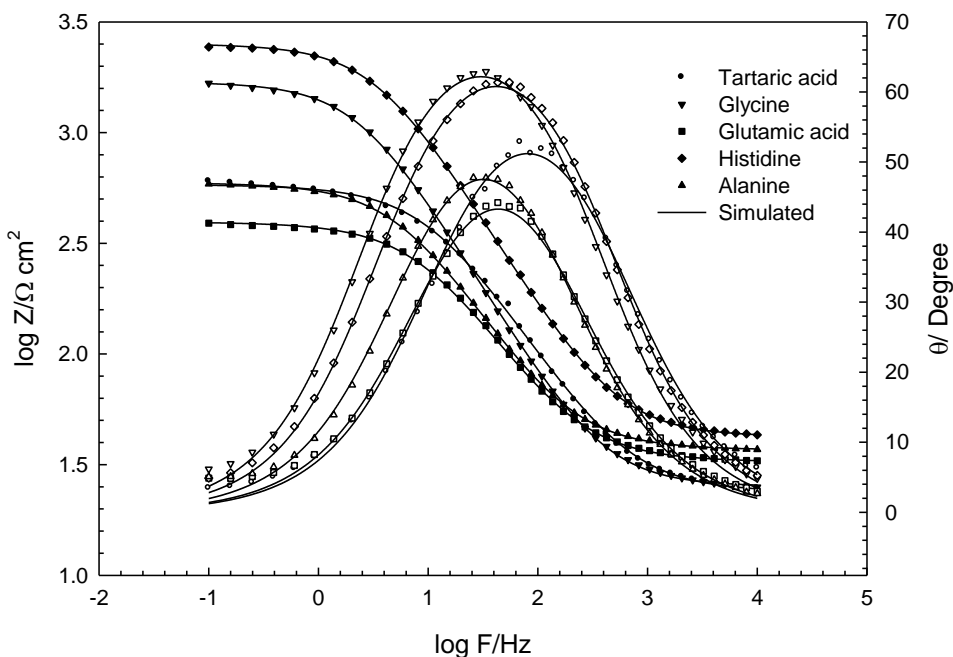


Figure 6. Bode plots for Sn electrode after 2 h immersion in amino acid free and 0.02 mol dm⁻³ amino acid containing tartaric acid (1.0 mol dm⁻³) solutions at 25°C.

Table 4. Equivalent circuit parameters for Sn electrode after 2 h immersion in 1.0 mol dm⁻³ aqueous tartaric acid solution containing 0.02 mol dm⁻³ of the different amino acids at 25°C.

[Amino Acid]	R _s (Ω)	R _{ct} (kΩ cm ²)	C _{dl} (μF cm ⁻²)	α
-	76.55	0.56	10.45	0.80
Glycine	81.03	1.671	14.50	0.84
Alanine	118.8	0.58	18.29	0.80
Histidine	136.0	0.59	16.89	0.83
Glutamic Acid	104.9	0.57	18.30	0.79

3.3. Adsorption isotherm

It is essential to know the mode of adsorption and the adsorption isotherm that fits the experimental results. Many attempts have been made to fit the surface coverage data to different adsorption isotherms. The adsorption isotherm for glycine, as a representative example of the investigated amino acids was investigated. The corrosion inhibition efficiency of glycine reached about

70 % at a concentration of 0.02 mol dm^{-3} and its adsorption on the metal surface was found to obey the Freundlich isotherm, according to:

$$\theta = KC^n \quad (9)$$

where C is the equilibrium concentration of the amino acid, n is a constant depending on the characteristics of the adsorbed molecule, where $0 < n < 1$, K is the equilibrium constant for adsorption/desorption process and θ is the fraction of the surface coverage [32]. The value of θ was calculated from the corrosion inhibition efficiency, σ , as being equal to:

$$\theta = \sigma \times 10^{-2} \quad (10)$$

K is related to the free energy of adsorption, ΔG , according to:

$$K = 1/C_{\text{solvent}} \exp(-\Delta G/RT) \quad (11)$$

where, C_{solvent} is the molar concentration of the solvent, which is 55.5 mol dm^{-3} for aqueous solutions. The logarithmic form of this isotherm is given by:

$$\log \theta = \log K + n \log C \quad (12)$$

This linear relation can be used for the calculation of the values of both K and n for the inhibitor used.

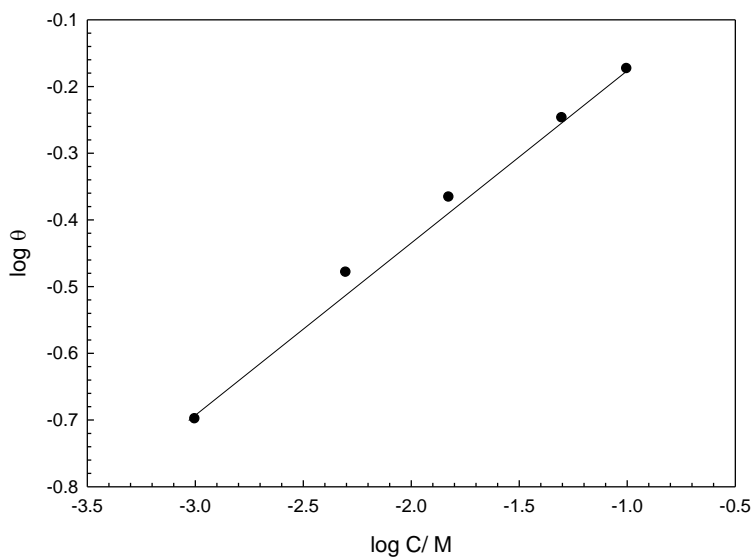


Figure 7. Adsorption isotherm for Sn in naturally aerated aqueous 1.0 mol dm^{-3} tartaric acid solutions containing different concentrations of glycine at 25°C .

The adsorption isotherm for the adsorption of glycine on tin in tartaric acid solution is presented in Fig. 7. The free energy of adsorption, ΔG , was calculated and has a value of $-10.2 \text{ kJ mol}^{-1}$, which reveals a physisorption controlled mechanism for the adsorption of glycine on the metal surface.

3.4 SEM measurements

Fig. 8 shows the surface morphology of tin surface before and after immersion in the different solutions.

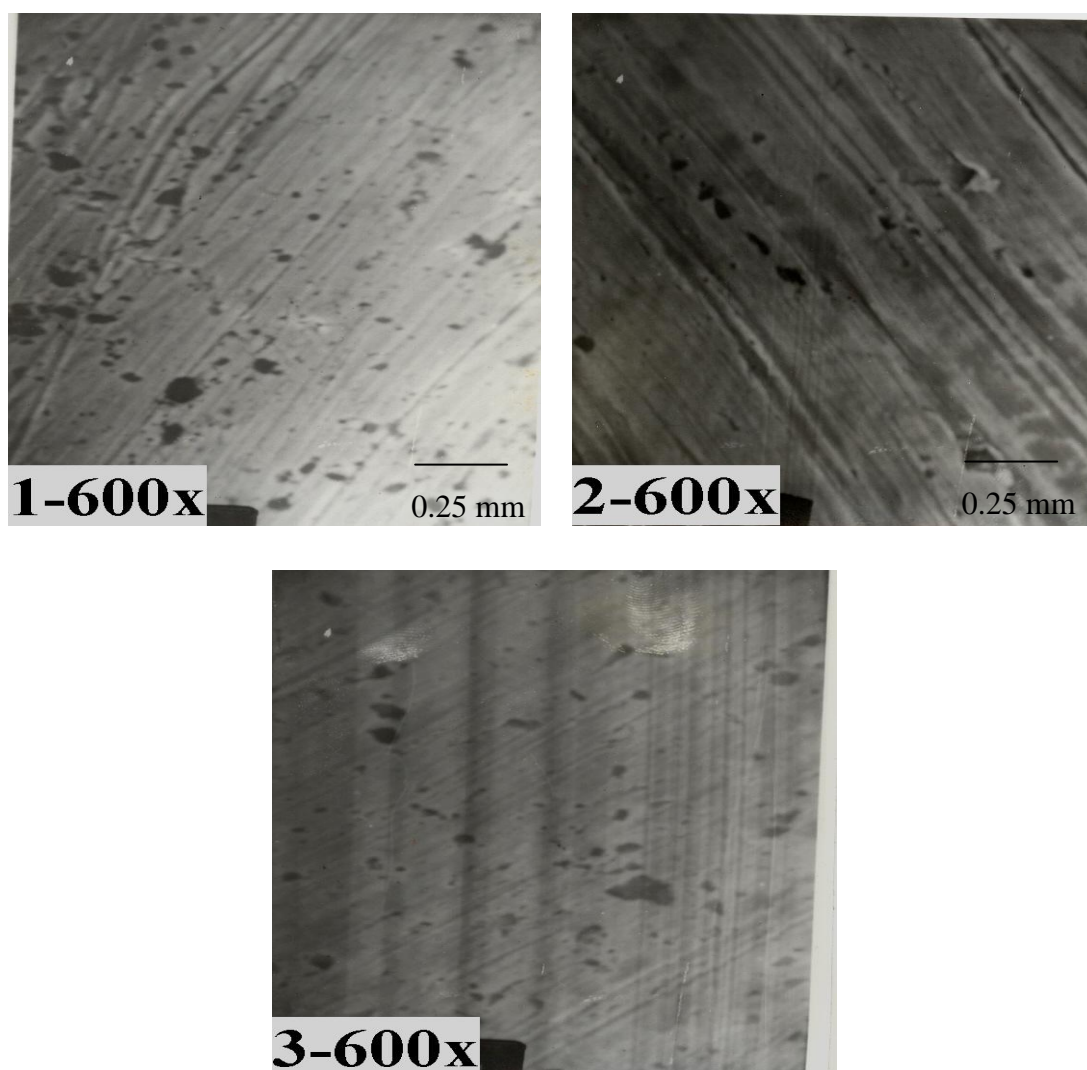


Figure 8. SEM images of: 1- Mechanically polished tin surface. 2- The metal surface after 2 h immersion in amino acid free naturally aerated 1.0 mol dm^{-3} aqueous tartaric acid solution at 25°C . 3- The metal surface after 2 h immersion in naturally aerated 1.0 mol dm^{-3} aqueous tartaric acid solution containing 0.02 mol dm^{-3} glycine at 25°C .

Fig. 8-1 shows the polished tin surface and Fig. 8-2 shows the same surface after 2 h immersion in an amino acid free aqueous tartaric acid solution. It is clear from the dark spots that the surface is subjected to corrosion. After tin immersion in the same solution to which 0.02 mol dm^{-3} glycine (Fig. 8-3) for the same time, the metal surface became smoother and the flawed regions were repaired.

4. CONCLUSIONS

Tin metal exhibits an active/passive transition, where the Sn(II) species undergo subsequent oxidation to the Sn(IV). The passivation of the tin surface is due to precipitation of a thin film of Sn(OH)_4 which transforms to an adherent stable film of $\text{SnO}_2 \cdot \text{H}_2\text{O}$.

- The presence of tartarate ions in the aqueous solution enhances the corrosion of tin, due to the adsorption of tartarate ion, which accelerates active dissolution.

- The addition of small amount of naturally occurring amino acids, e.g. 0.02 mol dm^{-3} glycine to the tartaric acid solution decreases the corrosion rate of tin up to 30% of its initial value. The mechanism of the corrosion inhibition process is based on the adsorption of the amino acid on the active corrosion sites of the metal surface.

- The adsorption of glycine follows the Freundlich adsorption isotherm and the free energy of adsorption was calculated to be -10.2 kJ/mol which reveals physical adsorption.

ACKNOWLEDGEMENT

The authors are grateful to the Alexander von Humboldt (AvH) foundation and Cairo University for providing the electrochemical work station.

References

1. S. Blunden, T. Wallace, *Food and Chemical Toxicology* 41 (2003) 1651.
2. R.P.G. Elbourne, G.S. Buchanan, *J. Inorg. Nucl. Chem.* 32 (1970) 493 and 3559.
3. H. Leidheiser Jr., A.F. Hauch, E.M. Ibrahim, R.D. Granata, *J. Electrochem.Soc.* 129 (1982) 1651.
4. B.F. Gannetti, P.T. Sumodjo, T. Rabockai, A. Souza, J. Barboza, *Electrochim. Acta* 37(1992) 143.
5. B.F. Gannetti, P.T. Sumodjo, T. Rabockai, A, *J. Appl. Electrochem.* 20 (1990) 672.
6. P.G. Smith, V.G. Kumar Das, "Tin relation to toxicity", P.G. Kumar Das Ed. Narosa Publishing House, New Delhi, India (1996).
7. M. Serugo, M. Metikos-Hukovic, T. Valla, M. Milun, H. Hoffschultz, K. Wandelt, *J. Electroanal. Chem.* 407 (1996) 83.
8. C.M.V. Almeida, B.F. Giannetti, T. Rabockai, *J. Appl. Electrochem.* 29 (1999) 123.
9. C.M.V. Almeida, B.F. Giannetti, *Mater. Chem. Phys.* 69 (2001) 261.
10. A.S. Tselesh, *Thin Solid Films* 516 (2008) 6253.
11. A.C. Clark, P.D. Prenzler, G.R. Scollary, *Food Chem.* 102 (2007) 905.
12. C.Y. Chan, K.H. Khoo, Y.C. Chua, S. Guruswamy, *Br. Corros. J.* 28 (1993) 53.
13. P.E. Avarez, S.B. Ribotta, M.E. Folker, C.A. Gervasi, J.R. Vilche, *Corros. Sci.* 44 (2002) 49.
14. W.A. Badawy, F..M.Al-Kharafi., A.S.El-Azab. *Corros. Sci.* 41 (1999) 709.

15. R.M. El-Sherif, K.M. Ismail, W.A.Badawy *Electrochim. Acta* 49 (2004) 5139.
16. W.A. Badawy, K.M. Ismail, A. M. Fathi, *Electrochimica Acta* 50 (2005) 3603.
17. P. Marsal, *Chimique et Toxicologique* 855 (1987) 71.
18. M.S.S. Morad, A.A.A. Hermas, *J. Chem. Technol. Biotechnol.* 76 (2001) 401.
19. CRC Handbook of Chemistry and Physics, 66th ed. 1985-1986.
20. A.E. Smith, *Analyst* 98 (1973) 209.
21. B.N. Stirrup, N.A. Hampson, *Surface and Coatings Technol.* 5 (1977) 429.
22. H. Döring, J. Garcke, W. Fisher, K. Wiesener, *J. Power Sources* 28 (1989) 367.
23. S.S. Abd El Rehim, H.H. Hassan, N.F. Mohamed, *Corros. Sci.* 46 (2004) 1071.
24. J.R. Macdonald, *Impedance Spectroscopy*, John Wiley & Sons. New York (1987).
25. W.A. Badawy, S.S. El-Egamy, K.M. Ismail, *Br. Corr. J.* 28 (1993) 133.
26. W.A. Badawy, F.M. Al-kharafi, *Electrochim. Acta* 42 (1997) 579.
27. K. Hladky, L.M. Dawson, *Br. Corr. J.* 15 (1980) 20.
28. J. Hitzig, J. Titz, K. Juettner, W.J. Lorenz, E. Schmidt, *Electrochim. Acta* 29 (1984) 287.
29. A.E Bohe, J. R Vilche, K. Juettner, W. J. Lorenz, W. Paatsch, *Electrochim. Acta* 34 (1989) 1443.
30. G. Bereket, A. Yurt, *Corros. Sci.* 43 (2001) 1179.
31. E. Stupnisek-Lisac, A. Gazivoda, M. Madzarac, *Electrochim. Acta* 47 (2002) 4189.
32. P.W. Atkins, *Physical Chemistry*, 5th ed., Oxford University Press. Oxford, (1994) 877.